Journal of Physiology (1989), **417**, *pp.* 83–103
With 9 text-figures
Printed in Great Britain

VOLTAGE-ACTIVATED CURRENTS RECORDED FROM RABBIT PIGMENTED CILIARY BODY EPITHELIAL CELLS IN CULTURE

BY GORDON L. FAIN AND NASSER A. FARAHBAKHSH*

From the Department of Ophthalmology, the Jules Stein Eye Institute, University of California School of Medicine, Los Angeles, CA 90024, USA

Received 17 January 1989

SUMMARY

1. The whole-cell recording mode of the patch-clamp technique was used to investigate the presence of voltage-activated currents in the isolated pigmented cells from the rabbit ciliary body epithelium grown in culture.

2 In Ringer solution with composition similar to that of the rabbit aqueous humour, depolarizing voltage steps activated a transient inward current and a delayed outward current, while hyperpolarization elicited an inwardly rectified current.

3. The depolarization-activated inward current was mainly carried by Na^+ and was blocked by submicromolar concentrations of tetrodotoxin. This current in many cells was sufficiently large to produce a regenerative Na^+ spike.

4. The depolarization-activated outward current was carried by K^+ and blocked by external TEA and Ba^{2+}. Its activation appeared to be Ca^{2+}-independent.

5. The hyperpolarization-activated inward current was almost exclusively carried by K^+ and was blocked by Ba^{2+} and Cs^+. For large hyperpolarizations below -120 mV, this current exhibited a biphasic activation with a fast transient peak followed by a slower sag, that appeared to be due to K^+ depletion.

6. The voltage-dependent K^+ conductances probably act to stabilize the cell membrane resting potential and may also play a role in ion transport. The function of the Na^+-dependent inward current is unclear, but it may permit the electrically coupled epithelial cells of the ciliary body to conduct propagated action potentials.

INTRODUCTION

The ciliary body epithelium is responsible for the formation of the aqueous humour in the eye (Bill, 1973). It consists of two cell layers: the pigmented cells, which lie directly adjacent to the stroma, and the non-pigmented cells, whose basal membranes face the posterior chamber (or lumen). These two cell layers are coupled by an extensive series of gap junctions at their apical membranes (Raviola & Raviola, 1978; Green, Bountra, Georgiou & House, 1985) and probably function together to pump ions and water from blood to the posterior chamber (Cole, 1984). The function of these cells has been difficult to study, partly because of the complicated

* To whom correspondence should be addressed. Authors' names are in alphabetical order.

MS 7461

morphology of the ciliary body. The pigmented cells, in particular, lie underneath the non-pigmented cells adjacent to the ciliary capillaries and are normally inaccessible. However, these cells are probably of great importance to the function of the ciliary epithelium, since they may be the site of receptors for peptides, hormones, and other substances (see for example Bianchi, Anand-Srivastava, De Lean, Gutkowska, Forthomme, Genest & Cantin, 1986).

Earlier transport studies (Chu, Candia & Iizuka, 1986) and intracellular recordings on the intact ciliary body epithelial tissue (Green *et al.* 1985), as well as recordings from confluent cell culture preparations of bovine pigmented cells (Helbig, Korbmacher & Wiederholt, 1987), have shown the presence of a K^+ conductance in this epithelium, which is Ca^{2+}- and pH-dependent and is blockable by Ba^{2+} (Helbig *et al.* 1987). In order to investigate the physiology of the pigmented cells in detail, we have developed a method for maintaining isolated rabbit pigmented ciliary body epithelial cells *in vitro* in tissue culture and for recording from them using patch-clamp techniques. Our results indicate that these cells possess at least three voltage-activated conductances similar to those usually seen in excitable tissues. Preliminary accounts of this work have been given (Farahbakhsh, Fain & Fain, 1987).

METHODS

Tissue culture

Young adult pigmented rabbits, approximately 9 weeks old, weighing 2–2·5 kg, were killed with a lethal injection of chloral hydrate or sodium pentobarbitone. After the animal had expired, the eyes were rapidly enucleated and washed in sterile balanced salt solution (BSS, Table 1). The globes were hemisected posterior to the ora serrata and the posterior segment was removed. The anterior segment was pinned onto the substrate of a dissecting dish which was filled with sterile BSS and placed on a slide warmer to maintain the tissue at 37 °C. The dissecting dish consisted of a 55 mm Petri dish containing a 5 mm layer of hardened Sylgard (Dow Corning, Midland, MI). The lens and residual lens capsule were carefully removed. To free the ciliary body from the iris, an incision was made at the border between the iridial and ciliary processes completely circumventing the iris. A second incision was made through the pars plana, and the ciliary body ring was then separated from the remaining cornea and sclera.

To obtain a pure preparation of epithelial cells, we removed the epithelium from the stroma, using the method of Cilluffo, Fain, Farahbakhsh, Fain & Lee (1988), as follows. The ciliary body ring was cut into several pieces, rinsed in sterile BSS, and then incubated for 35 min in Ca^{2+}- and Mg^{2+}-free BSS (CMF-BSS, Table 1) containing 2·4% dispase (Grade 2, Boehringer Mannheim, Indianapolis, IN) with 100 mM-sorbitol (Sigma, St Louis, MO). After rinsing in CMF-BSS, the epithelium was carefully dissected from the underlying stroma.

The epithelial pieces were then washed and placed in growth medium consisting of minimal essential medium (MEM) with Earle's salts and L-glutamine (GIBCO, Grand Island, NY), to which was added 20% fetal bovine serum (FBS), 3 mM-L-glutamine, gentamicin (50 μg/ml), and kanamycin (50 μg/ml). The pieces of epithelium were triturated through a narrow-bore glass pipette, and the resulting cell suspension, containing both pigmented and non-pigmented cells, was plated onto 35 mm plastic Petri dishes, whose bottoms had been replaced by glass cover-slips. These Petri dishes were then placed in a 37 °C incubator with an atmosphere of 5% CO_2 in air.

Superfusion system and solutions

The modified Petri dishes used for growing cells were placed on the stage of an inverted microscope (Invertoscope D, Carl Zeiss, Oberkochen, FRG) and used as the recording chamber. The experiments were performed at room temperature (20–22 °C). Cells were continuously superfused with Ringer solution (Table 1) or one of the test solutions. The composition of the Ringer solution was chosen to be similar to that of the aqueous humour of the rabbit (Cole, 1984). Tetrodotoxin

(TTX, Sigma; final concentration 30 or 200 nM) and tetraethylammonium chloride (TEA-Cl, Sigma; 10 mM) were added directly to the Ringer solution before each experiment. For solutions containing $BaCl_2$ (2 mM) we found it necessary to replace the $MgSO_4$ in the Ringer solution with $MgCl_2$ to prevent precipitation of $BaSO_4$. The Na^+-free Ringer solution was made by substituting tetramethylammonium chloride (TMA-Cl) for NaCl and choline bicarbonate for $NaHCO_3$ in the Ringer solution on a mole-for-mole basis. Osmolality (see Table 1) was measured with a vapour pressure osmometer (models 5100B and 5500; Wescor, Logan, UT).

TABLE 1. Solutions

	BSS*	CMF–BSS*	Ringer soln†	Internal soln‡
NaCl	127	127	111	10
$NaHCO_3$	14	14	35	—
Na_2HPO_4	1·08	1·08	—	—
KCl	3·8	3·8	4·3	130
KH_2PO_4	0·6	0·6	—	—
$CaCl_2$	0·31	—	1·7	0·5
$MgSO_4$	0·63	—	0·8	2
D-Glucose	6·1	6·1	7	—
Sucrose	—	—	10	—
EGTA	—	—	—	5·5
HEPES-KOH	—	—	—	10
pH (at 37°)	7·5	7·5	7·4	7·1
Osmolality	268	266	294·5	296·6

* BSS and CMF–BSS also contained 0·0005 % Phenol Red and were bubbled with 5 % CO_2/95 % O_2 mixture. Osmolalities given are average of five measurements on samples made at different dates.

† Ringer solution was continuously bubbled with 5 % CO_2/95 % O_2 mixture. Osmolality given is the average of eleven solutions.

‡ 1·5 mM-ATP and 0·1 mM-GTP were added to the internal solution before use. Calculated free Ca^{2+} concentration was $1{\cdot}4 \times 10^{-8}$. Osmolality given is average of three solutions.

The solution superfusing the cells was altered with a solenoid which activated a remote-controlled pneumatic valve. This valve was in turn mechanically coupled to a four-way flow valve (Hamilton Co., Reno, NV), which was arranged so that as one solution was flowing to the chamber, another was passing to a waste container. In this way it is possible to change solutions quickly and to superfuse the cells with different solutions without any interruption in the flow (see Hodgkin, McNaughton, Nunn & Yau, 1984). The flow rate was 1 ml/min and the dead space between the four-way valve and the chamber was 200 μl. The chamber volume was 1 ml.

Recording electrodes

Patch-clamp electrodes were pulled from borosilicate glass micropipettes with filament (Sutter Instrument Co., San Rafael, CA) on a programmable Flaming-Brown puller (model P80/PC; Sutter Instrument Co., San Rafael, CA) to a final tip diameter of 1–2 μm and immediately used. The pipettes were not coated or fire-polished. The electrodes used in these experiments were filled with internal solution (Table 1) and had a resistance of 2–4 MΩ. Typical seals had a resistance in the range of 1–5 GΩ, though seals with resistances larger than 10 GΩ were occasionally formed. The bath was grounded through an agar bridge–Ag–AgCl electrode. The junction potentials between the bath and tips of both ground and patch-clamp electrodes were measured independently for all solutions, and appropriate corrections in membrane potentials have been made. Measurements of junction potentials were made with a reference electrode filled with high concentration (3–5 M) of KCl or CsCl (Hagiwara & Ohmori, 1982; Fenwick, Marty & Neher, 1982).

Electrical recordings

The whole-cell configuration of the patch-clamp technique (Hamill, Marty, Neher, Sakmann & Sigworth, 1981) was used to investigate macroscopic currents activated by voltage steps. Currents

were recorded using a List patch-clamp amplifier (model L/M-EPC 7, List-Electronics, Darmstadt, FRG), with the current signal filtered at 3 kHz. Analog compensation of cell and electrode capacitance and series resistance (up to 70%) was utilized during recordings to minimize the capacitive transient in the current records and the error in the applied command potential. Both voltage and current signals were digitized at 44 kHz with 16-bit resolution by a digital audio processor (model 701–ES; Sony Corp. of America, Park Ridge, NJ), modified as by Bezanilla (1985), and recorded on a video cassette recorder (model SL-2700; Sony). The recorded data could be played back in digital form into an IBM PC-AT computer (International Business Machines Corp., Boca Raton, FL) for analysis. Holding and command potentials were generated by the same computer under software control and delivered to the amplifier command input through a digital-to-analog convertor (model PCM 53JGI; Burr-Brown Corp., Tucson, AZ). Command potentials were generally 30 ms long and applied at 2 Hz, unless otherwise noted. A brief account of the original design of the hardware and software used here for signal generation, data acquisition and analysis is given by Stimers, Bezanilla & Taylor (1987). Inward currents are shown downward in all figures.

Cell input resistance and membrane capacitance

In order to determine the cells' input resistance (R_{in}), membrane capacitance (C_m), and access (series) resistance (R_a), uncompensated current responses to 10 mV voltage steps from a holding potential of −60 mV were recorded (Lindau & Neher, 1988). Ten or more such current records were averaged and fitted with the sum of exponential functions using a least-square-error curve fitting routine. Number of crossings (N_c), or number of times the quantity 'measured value minus model prediction' changed sign, was used as an indicator for the goodness of fit. The fit with the smallest number of exponential terms which satisfied the relation $N_c > N_p/10$, where N_p is the number of sampled points, was accepted (see Fig. 1).

The transient responses of thirty cells were fitted with the sum of exponential terms. These successful fits indicated that within the voltage range in which no voltage-dependent conductances were activated, the cells could be modelled as lumped passive R–C networks. For eight cells, two or more exponential terms were needed for satisfactory fits (not shown). However, for the remaining twenty-two cells, the transient responses could be fitted with a single exponential (Fig. 1), suggesting an equivalent circuit composed of a parallel combination of a capacitor (C_m, Fig. 1, inset) and a resistor (R_m) in series with another resistor (R_a). The fitted single-exponential curve is given as:

$$i(t) = i_{ss} + (i_0 - i_{ss})\, e^{-t/\tau}, \tag{1}$$

where $i(t)$ is the predicted current at time t after the onset of the voltage step; i_{ss}, the steady-state current; i_0, the initial current obtained by extrapolating the exponential fit to the time of the voltage step onset; and τ, the time constant. The parameters R_a, R_m and C_m could then be estimated from:

$$\left.\begin{aligned} R_a &= V_0/i_0 \\ R_m &= V_0/i_{ss} - R_a \\ C_m &= \tau/(R_a \parallel R_m), \end{aligned}\right\} \tag{2}$$

where V_0 is the voltage step amplitude and the symbol $\parallel$ is used to indicate a parallel combination. For the cell in Fig. 1, $R_a = 7{\cdot}8 \times 10^6\ \Omega$, $R_m = 9{\cdot}4 \times 10^8\ \Omega$, $\tau = 0{\cdot}53$ ms and $C_m = 68$ pF. Assuming a specific membrane capacitance of 1 μF/cm^2 and an isopotential cell membrane (see below), we found a specific membrane resistance, $R_M = 64\ \text{k}\Omega\ \text{cm}^2$.

It should be noted that R_m in this model corresponds to the parallel combination of the cell input resistance, R_{in}, and the pipette-membrane seal resistance, R_{seal} (Fenwick *et al.* 1982; Tessier-Lavigne, Attwell, Mobbs & Wilson, 1988). Thus,

$$R_{in} = R_{seal} R_m/(R_{seal} - R_m) \tag{3}$$

Hence, $R_{in} > R_m$. Therefore, R_m should be considered an underestimate or lower bound for R_{in}. Only when R_{seal} is much larger than R_{in}, can R_m be taken as a reasonable estimate of R_{in} (Marty & Neher, 1983). We could not measure or calculate the pipette–membrane seal resistance in the whole-cell clamp mode (Lindau & Neher, 1988). However, the apparent seal resistance (R_{app}), measured in the on-cell mode, can be used as an estimate for R_{seal}. The term R_{app} is itself the resistance of a parallel combination of R_{seal} and $R_p + R_{in}$, where R_p is the resistance of the membrane patch (Fischmeister,

Ayer & DeHaan, 1986). Hence, $R_{app} < R_{seal}$. Therefore, substituting R_{app} for R_{seal} in eqn (3) leads to an overestimate or upper bound for R_{in}. An implied assumption in this analysis is that R_{seal} remains unchanged during the transition from the on-cell to whole-cell mode. After some of our whole-cell recordings we excised the membrane by pulling the electrode away from the cell and forming an outside-out patch. In such cases we found that the measured seal resistance was within

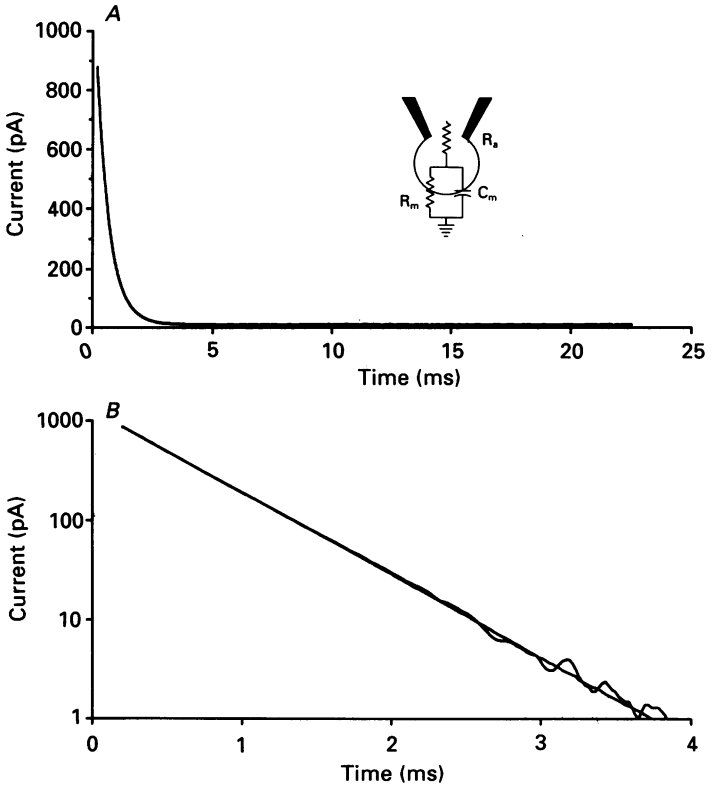

Fig. 1. *A*, the transient current response of a cell to a 10 mV voltage step recorded with the patch-clamp amplifier in voltage clamp mode with no capacity compensation. Also shown is the single-exponential fit with time constant, $\tau = 0{\cdot}526$ ms. Because of the closeness of the fit, the two curves cannot be distinguished. Number of crossings, $N_c = 113$; number of sampled points, $N_p = 1015$. *B*, semilogarithmic plot of decay segment of the transient current and exponential fit shown in *A*, after subtraction of the steady-state value of the current i_{ss}. These plots indicate that, despite the spindle-like shape of this cell, its uncompensated small-signal transient response could be fitted reasonably well with a single-exponential function. Thus, the passive properties of the cell-pipette combination can be modelled with an R–C circuit, as shown in the inset of *A*. Using the parameters of the exponential fit and assuming an infinite resistance for the cell-pipette seal (see text), we determined R_a to be 7·8 MΩ, R_m to be 940 MΩ, and C_m to be 68 pF. Recording bandwidth for this and the rest of the Figures was 0–3 kHz. See text for definitions of symbols.

25% of the one measured in the on-cell mode. For the cell in Fig. 1, R_{app} was 2 GΩ. Thus, the upper limit for the input resistance was $1{\cdot}8 \times 10^9$ Ω. The upper bound for the specific membrane resistance was 120 kΩ cm².

Of the twenty-two cells whose small voltage-step response could be fitted with a single exponential, one cell had a large time constant (1·7 ms), because of a large series resistance (24·8 MΩ), and two had small input resistances (50 MΩ or less). As the following analysis will show, both

a large series resistance and a small input resistance are detrimental to maintaining the space and voltage clamp required for recording voltage-activated currents. Therefore data recorded from such cells were not used. A summary of the parameters measured for the remaining nineteen cells is given in Table 2. The estimated membrane surface area varied from 1950 to 8800 μm^2 (6170 $\pm$ 2230 μm^2, mean $\pm$ S.D., $n = 19$), while the areas calculated from the pigmented ciliary body

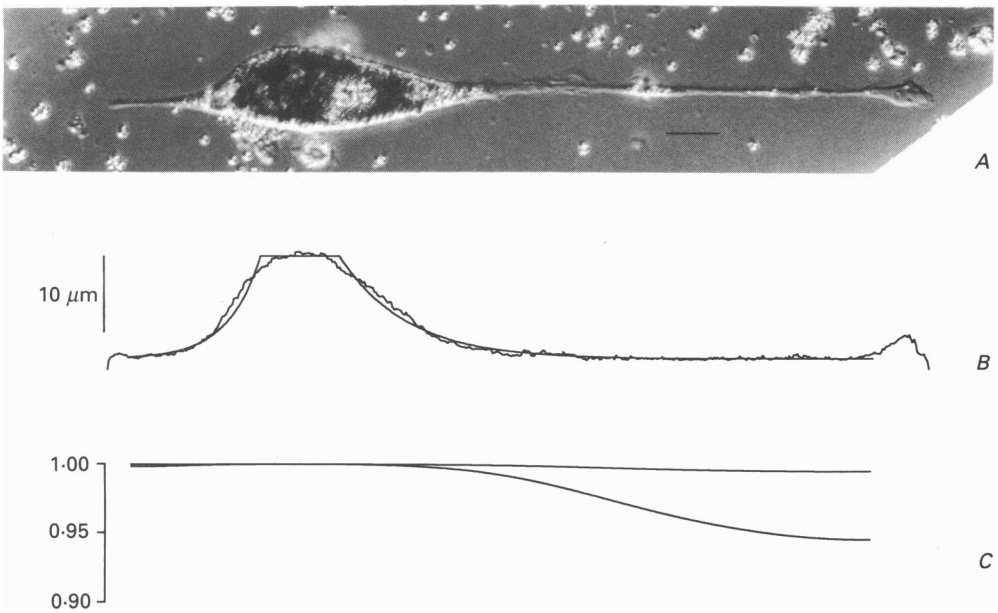

Fig. 2. *A*, a single isolated pigmented ciliary body epithelial cell, photographed using differential interference contrast (DIC) optics. Horizontal bar is 10 μm. *B*, variation in the diameter of the cell's two processes is plotted against distance from the soma (jagged trace) and has been fitted with two exponential curves (smooth traces). Vertical bar is 10 μm. Horizontal scale is the same as in *A*. *C*, the transmembrane voltage along the length of the cell in *A*, expressed as fraction of the amplitude of the voltage step applied at the soma, was obtained by assuming that the cell processes taper exponentially as shown in *B*. The curves shown are the steady-state solutions of the cable equation (Jack *et al.* 1975) for (in μm): $d_0 = 15{\cdot}17$, $d_\infty = 1{\cdot}42$, $b_{right} = 12{\cdot}5$, $b_{left} = 6{\cdot}25$, $l_{right} = 100$ and $l_{left} = 25$. A value for R_i was chosen as 100 Ω cm and $R_M = 10$ kΩ cm^2 for upper curves and 1 kΩ cm^2 for lower curves. Horizontal scale is the same as in *A*. See the text for the definition of symbols.

epithelial (PCE) cell images (e.g. 2160 μm^2, Fig. 2*A*), lie within this range but toward the lower end (almost three times smaller than the mean), and the area calculated for a $20 \times 10 \times 10$ μm^3 PCE cell (Green *et al.* 1985) is even smaller. This discrepancy may result from the membrane infoldings in both intact and cultured cells. Our estimate of the specific membrane resistance (Table 2) are on average an order of magnitude larger than that used by Green *et al.* (1985), which was based on the measurements in *Necturus* gall-bladder (Frömter, 1972).

Adequacy of space and voltage clamp

Quantitative interpretation of currents recorded under voltage clamp relies upon the assumption of isopotentiality in both time ('voltage clamp') and space ('space clamp'). Pigmented ciliary body epithelial cells grown in culture have somas between 10 and 20 μm in diameter and processes which can be over 100 μm long (see Fig. 2*A*). The surface area of these cells (estimated from membrane capacitance measurements) can be as large as 9×10^3 μm^2, almost 10 times larger than for

chromaffin cells (Fenwick *et al.* 1982). For this reason, we have investigated the quality of the space clamp by estimating the voltage drop along the processes of some typical PCE cells. We have also determined maximum permissible current for which the voltage drop across the access resistance remains below an acceptable level.

To measure variations of cell diameter as a function of the distance from the soma, several

TABLE 2. Summary

	Mean ± S.D.	Range
Access (series) resistance, R_a	9·4 ± 3·7 MΩ	5·3–16·5 MΩ
Input resistance (lower bound), R_m	670 ± 569 MΩ	111·5–2247 MΩ
Input resistance (upper bound), R_{in}	1·1 ± 1·1 GΩ	118–4080 MΩ
Specific resistance (lower bound), R_M	40 ± 34 kΩ cm²	5·4–127 kΩ cm²
Specific resistance (upper bound)	68 ± 76 kΩ cm²	5·7–260 kΩ cm²
Time constant, $\tau = (R_a \parallel R_m)C_m$	0·52 ± 0·17 ms	0·2–0·82 ms
Membrane capacitance, C_m	61·7 ± 22·3 pF	19·5–88 pF

Values given are mean ± S.D. and range for nineteen cells. See text for method of measurement and calculation. The values for R_a and C_m which were read directly from the G-SERIES and C-SLOW knobs of the List amplifier after compensating the cells' capacitance, were generally within 10% of those obtained as the result of curve fitting.

typical cells were photographed using differential interference contrast optics. The cells' images were captured from the printed photographs with a Sony video camera, digitized using a frame grabber (model DT2861, Data Translation, Marlboro, MA), and stored on the computer hard disc (model Vectra RS/20; Hewlett Packard, Sunnyvale, CA). Each image was later displayed on a video monitor (model PVM-1271Q; Sony). Contrast profiles of the images along lines perpendicular to the axes of the processes were used to determine the outline of the cells. The diameter of the cross-section of each cell was plotted against distance from the cell soma (Fig. 2*B*), and these data were fitted with an exponential function

$$d(x) = d_\infty + (d_0 - d_\infty)\, e^{-x/b} \quad (4)$$

where $d(x)$ is diameter of the process at distance x from the soma; d_0, the initial diameter; d_∞, the final diameter for cylindrical segment of the process; and b, the length constant of the taper. Other functions (e.g. normal or hyperbolic functions) could be used as well, but in terms of the conclusions drawn here, the results were not significantly different.

The steady-state solution of the cable equation (Jack, Noble & Tsien, 1975, eqn 7.42) was found for exponentially tapered cables using a multiple-shooting method (IMSL Math/Library, 1987, IMSL Inc., Houston, TX). The solution was in the form of a voltage profile (Fig. 2*C*) for a given cable geometry, a given specific membrane resistance (R_M) and a given axial resistance (R_i). From this solution it was possible to calculate the injected current as well as the input resistance.

For the cell in Fig. 2, the parameters of the exponential fit were (in μm): $d_0 = 15{\cdot}17$, $d_\infty = 1{\cdot}42$, $b_{right} = 12{\cdot}5$, $b_{left} = 6{\cdot}25$, $l_{right} = 100$ and $l_{left} = 25$, where l is the length, and the subscripts right and left refer to the right and left processes. Figure 2*C* shows the voltage profile (steady-state solutions of the cable equation) assuming $R_i = 100\ \Omega$ cm, and $R_M = 1$ kΩ cm² (lower curve) or $R_M = 10$ kΩ cm² (upper curve). These results suggest that for $R_M > 10$ kΩ cm², the maximum voltage drop along the processes of this cell will be less than 0·6% of the voltage applied at the soma. For $R_M = 1$ kΩ cm², the maximum drop is approximately 6%. Using the smallest value of R_M found for the cells included in calculations for Table 2 (5·6 kΩ cm²), and the geometry of the cell in Fig. 2*A*, we obtained a maximum voltage drop of 1·1% of the applied voltage.

While these results were obtained for a cable with a constant membrane resistance (passive membrane), they are still applicable, to a first approximation, to a cable that has reached steady state after activation of a voltage-dependent conductance whose current–voltage curve has a positive slope (referred here as 'positive-slope conductance', e.g. the delayed rectifier) (Joyner, Moore & Ramone, 1975). Of course in such cases, a much lower R_M corresponding to that of the activated membrane should be used in the calculations. For the cell in Fig. 1, R_M was 64 kΩ cm²

(lower bound). Thus, activation of voltage-dependent (positive-slope) conductances can lower the specific membrane resistance by a factor of 64 (i.e. to 1 kΩ cm²) before the voltage level anywhere along the processes drops below 94% of that applied at the soma. This assumes that voltage-activated conductances are uniformly distributed. Similar limits can be found for other cells. Using the lower bounds for R_M in nineteen cells used for the calculations in Table 2, we found that the voltage-activated conductances in these cells can on average be as large as 39 times the passive (leakage) conductance. In other words, for a 100 mV step change in the membrane potential, up to 6 nA current can be induced in an average PCE cell without compromising the adequacy of the space clamp.

On the other hand, the adequacy of the space clamp during the transient activation phase of negative-slope conductances (e.g. the depolarization-activated inward current; see Results) cannot be deduced from the above analysis. This latter case would require estimation of the voltage drop along the processes of the cells during the transient phase of the inward current by finding the solution of the partial differential equation (i.e. cable equation) for a tapered cable with non-linear properties. Based on the results obtained for cylindrical cables (Taylor, Moore & Cole, 1960), however, we suspect that the more-or-less symmetrical shape of the depolarization-activated inward current recorded under whole-cell clamp (see Figs 6*A* and 7*B*) is indicative of a partial failure of the space clamp during the transient phase. This is due to what Taylor *et al.* (1960) have referred to as 'no-notch' error (their Fig. 22).

In addition to these difficulties, the effect of activation of large currents on the quality of the voltage clamp should also be considered. The access (or series) resistance measured for these nineteen cells was 9·4 ± 3·7 MΩ (Table 2). Usually, we compensated 50–70% of the access resistance electronically. This would leave, on average, 3·8 MΩ of the access resistance uncompensated. A maximum voltage drop of 6% (7·5 mV drop for a 120 mV voltage step) across the access resistance was considered acceptable (Marty & Neher, 1983). Therefore, we conclude that in most PCE cells, currents no larger than 2 nA could be activated (through positive-slope conductances) without adversely affecting the quality of voltage or space clamp. It should also be noted that because of the dynamic nature of the voltage-activated currents, the voltage drop across uncompensated part of R_a is 'time dependent' and thus cannot be corrected for after the recording has been made (Taylor *et al.* 1960). For this reason, we have indicated the *intended* voltage (command potential applied to the electrode) next to each current trace in our figures and have mentioned in the text and figure legends the cases where the voltage clamp conditions were unsatisfactory. Because of uncertainty about the adequacy of the space clamp during the full time course of activation of the voltage-dependent conductances, we have not attempted a detailed analysis of the kinetics of these currents.

RESULTS

During the first 24 h in culture, PCE cells adhered to the substrate and began to flatten and proliferate. The PCE cells were identified from their prominent perinuclear melanosomes and from the absence of staining of these cells with a monoclonal antibody which selectively stains the non-pigmented cells (Fain, Smolka, Cilluffo, Fain, Lee, Brecha & Sachs, 1988). Even though it has been shown that the cell layer which peeled off from the ciliary body after dispase treatment contains only epithelial cells (Cilluffo *et al.* 1988), and that our culture medium did not support growth of the non-pigmented cells (Cilluffo, Fain, Fain & Brecha, 1986), cells without melanin pigment granules were not used. Recordings were mostly made from single, isolated, spindle-shape, pigmented cells between 3 and 14 days after plating. A typical cell from which recordings were made is shown in Fig. 2*A*. No recordings were made from large flat cells or cells with apparent contact to neighbouring cells. During the course of these experiments a total of 436 cells were whole-cell clamped. Of these,

112 cells showed either small input resistance, a large time constant, or a multi-component capacitive transient that could not be successfully compensated with the amplifier's analog compensation circuitry. The data recorded from such cells were not included in this report.

Voltage-activated currents

Figure 3 illustrates the voltage-activated currents recorded from a PCE cell. These currents were activated by stepping the cell transmembrane potential for 30 ms from the holding potential of −60 mV to the levels indicated next to each trace. This cell appeared to have at least three different voltage-dependent conductances. In response to voltage steps to transmembrane potentials positive to −45 mV, a transient inward current could be observed (depolarization-activated inward current or DAIC). This current reached a maximum of 240 pA at 0 mV and then declined in amplitude with further depolarization. Lowering the holding potential to −80 mV more than doubled the size of the maximum current (not shown). Depolarizing voltage steps also activated a delayed outward current (depolarization-activated outward current or DAOC), which led to a net outward current for potentials positive to −20 mV. The net outward current in this cell grew to 840 pA at +80 mV. In response to hyperpolarizing voltage steps an inwardly rectified current was recorded. For voltages positive to −120 mV, this hyperpolarization-activated inward current (HAIC) was monophasic, but larger hyperpolarizations induced a biphasic current with a prominent 'sag' which became steeper with increasing transmembrane potential.

The maximum steady-state (chord) conductances activated by voltage in this cell, were 7 nS in response to depolarization to +20 mV and 24 nS for hyperpolarization to −120 mV. The maximum chord conductance activated transiently was 4 nS for DAIC and 28 nS for HAIC. Thus, the input resistance in this cell never fell below 36 MΩ, and the specific membrane resistance, assuming a uniform distribution of voltage-dependent conductances, remained above 2 kΩ cm^2 at all times. Therefore it appeared that, at least during the steady-state activation of these conductances, the voltage drop along the processes was less than 6% of the voltage applied at the soma. However, for voltages negative to −120 mV, the voltage drop across the access resistance exceeded 7·5 mV and thus the condition for voltage clamp was not met (see Methods). It should be mentioned, however, that the voltage drop across R_a is probably not responsible for the sag in these currents. If it can be assumed that the instantaneous conductance underlying the HAIC is monotonically increasing with hyperpolarization, the error in the command potential caused by R_a is of the wrong sign to produce the sag observed.

The three voltage-dependent currents we have described were not usually observed in the same cell (as in Fig. 3) but were more commonly seen singly or in combination with one other current. Of the three, DAOC was the most commonly recorded. All 324 cells from which acceptable recordings could be made (cells having a single-component capacitive transient, a short time constant, and a low leakage current) possessed the delayed outward current. The DAIC was recorded from eighty-two such cells (25·3%), while HAIC was seen in forty-three cells (13·3%). In

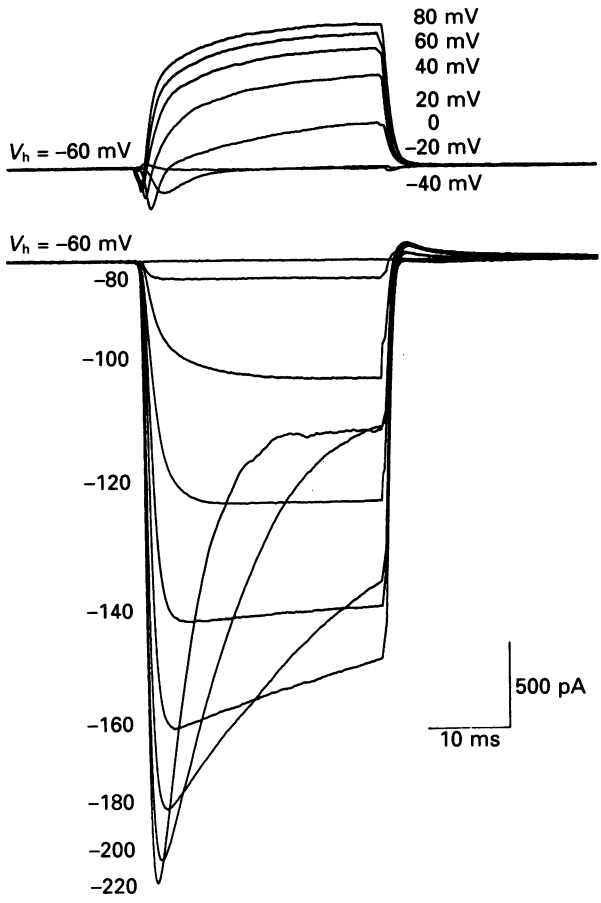

Fig. 3. Voltage-activated currents recorded from a PCE cell using the whole-cell clamp mode of the patch-clamp technique. Voltage pulses lasting 30 ms were applied at a frequency of 2 s^{-1}. Holding potential was −60 mV. Each trace is average of ten records. The value given next to each trace is the intended transmembrane potential during the voltage pulse. For this recording R_a = 5·3 MΩ, R_m = 262 MΩ, τ_m = 0·3 ms, C_m = 58·1 pF and R_M = 15·2 kΩ cm^2. The cell was superfused with the Ringer solution. See text for the definition of symbols.

all but four cells possessing HAIC, a sag of current at large hyperpolarizations was observed.

The depolarization-activated outward current is a K^+ current

Figure 4 shows depolarization-activated currents recorded from a pigmented ciliary body cell that lacked any noticeable DAIC. The cell was depolarized for 30 ms to transmembrane potentials from −40 to +60 mV. After recording the family of currents in normal Ringer solution (Fig. 4*A*), the bath was changed to Ringer solution to which 10 mM-TEA was added. As the solution change was made, responses to depolarizing steps to 0 mV were recorded (Fig. 4*B*). The TEA

suppressed the outward current. After 2 min, the size of DAOC was less than 10% of its initial level. It is likely that the time course of the TEA effect in this figure, as well as that in Fig. 4*D*, reflects the time course of the solution exchange in the recording chamber. The family of current responses recorded in the presence of TEA

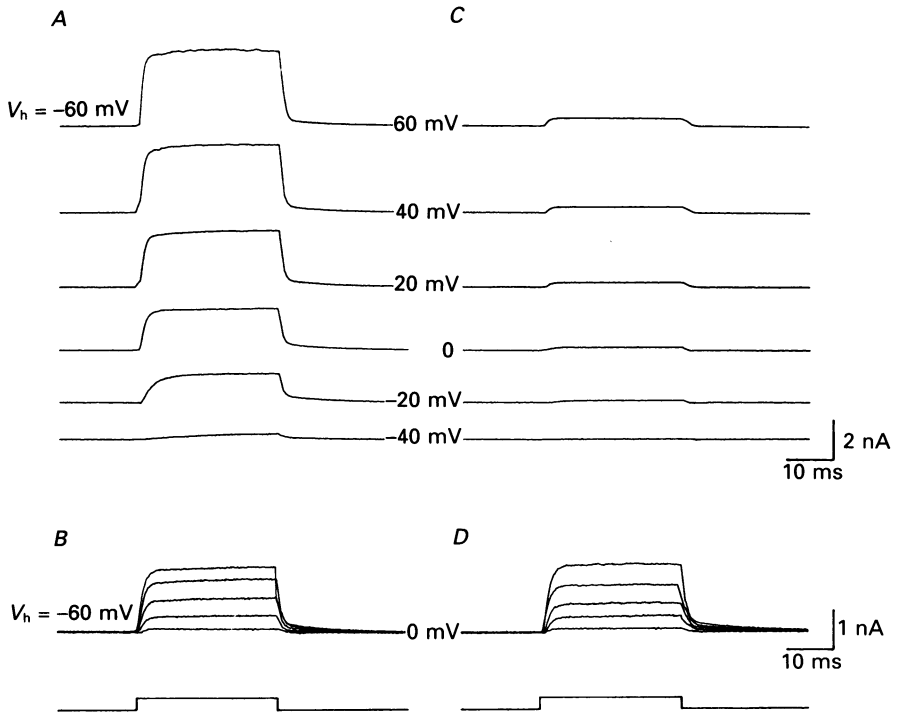

Fig. 4. Outward current is reversibly suppressed by 10 mM-TEA. Depolarization-activated outward currents were recorded from a PCE cell before (*A*) and after (*C*) addition of 10 mM-TEA to Ringer solution. Each trace is average of ten records. This cell lacked any observable depolarization-activated inward current. Transmembrane potential during each voltage step is shown next to the recorded responses. Holding potential was −60 mV. The time course of suppression of the outward current by TEA is shown in *B*. Here, all traces are currents activated by a 60 mV pulse (to 0 mV transmembrane potential), recorded at 30 s intervals during the onset of TEA superfusion. *D* shows recovery of the outward current during wash-out of TEA. Again, responses to 60 mV pulses recorded at 30 s intervals are shown. For this cell R_a = 9·1 MΩ, R_m = 446 MΩ, and C_m = 93 pF, and R_a was 60% compensated.

(Fig. 4*C*) shows that, within the range of potentials tested, the effect of TEA was voltage independent. Removal of the TEA led to gradual recovery of the DAOC (Fig. 4*D*). Similar results were obtained in five cells. The blocking effect of external TEA on the DAOC is similar to its effects on the delayed rectifier in the node of Ranvier, skeletal muscle and molluscan neurones (see Stanfield, 1983). External Ba^{2+} and internal Cs^+ (not shown) also reduced the size of the outward current.

The ionic selectivity of the depolarization-activated outward conductance was determined by recording tail currents (Fig. 5). The cell bathed in Ringer solution was initially held at −60 mV to remove inactivation, then depolarized to +40 mV for

30 ms to activate DAOC to its maximum extent, and finally brought to different potentials to record the tail current. As the inset in the Fig. 5 shows, the reversal potential for DAOC in this preparation was around −66 mV. Using the Goldman–Hodgkin–Katz equation, we obtained a selectivity for K^+ over Na^+, $P_{K/Na}$, of

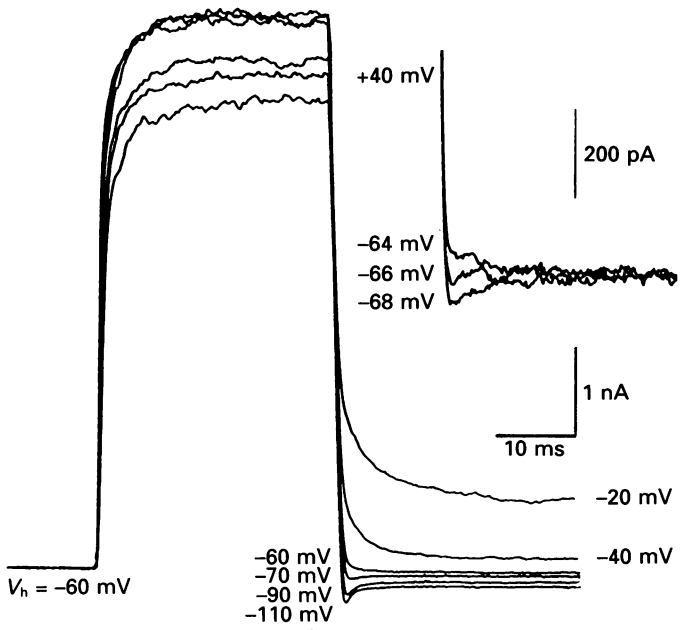

Fig. 5. Reversal potential of the DAOC from tail currents. The cell was initially held at −60 mV, then depolarized to +40 mV for 30 ms to activate all outwardly rectifying channels, and finally brought to potential levels between −110 and −20 mV. For the final voltage levels negative to −70 mV, the tail current became transiently inward (downward on the plot), while for potentials more positive than −60 mV, this current was outward. As is shown in the inset the reversal potential for the tail current in this cell was near −66 mV. In this recording R_a = 12·9 mΩ, R_m = 298 MΩ and C_m = 44·3 pF. The cell was superfused with the Ringer solution.

20. For five cells, $P_{K/Na}$ was 18·8 ± 1·3 (mean ± S.D.). The selectivity of DAOC for K^+ over Na^+ was therefore similar to that of the delayed rectifier currents recorded from other preparations (see Hille, 1984), including the voltage-dependent (and Ca^{2+}-independent) K^+ current in the basolateral membrane of rabbit urinary bladder ($P_{K/Na} > 10$, Lewis & Hanrahan, 1985).

The depolarization-activated inward current is carried mainly by Na^+

In addition to the DAOC, depolarization induced a transient inward current in some PCE cells superfused with Na^+-containing solutions. Figure 6*A* shows current recordings from one such cell for depolarizing voltage steps to −20 mV from a holding potential of −80 mV. In the Na^+-containing Ringer solution, depolarization elicited a net inward current (trace Na^+ in Fig. 6*A*), which became outward when external Na^+ was replaced by TMA (trace TMA) and completely disappeared when 200 nM-TTX was added to the Na^+-containing Ringer solution (trace TTX). The transient *outward* current is likely to be carried by internal Na^+ (10 mM, Table 1) and

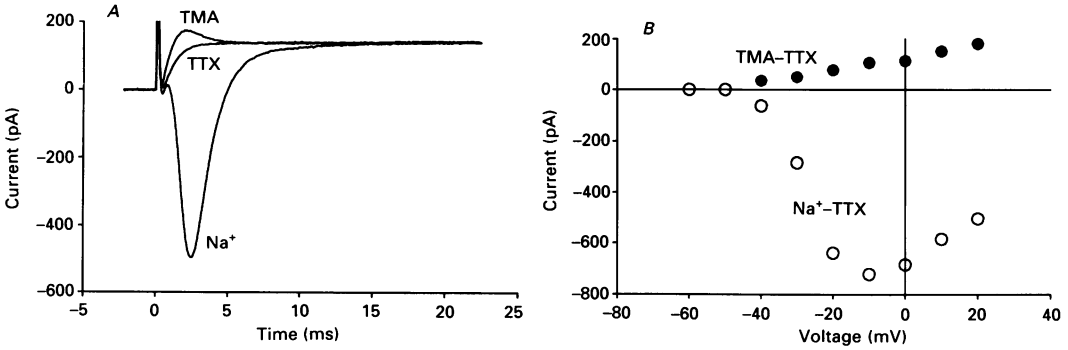

Fig. 6. *A*, the DAIC is a TTX-blockable Na^+ current. Depolarization-activated currents recorded from a PCE cell in response to 60 mV voltage steps from a holding potential of −80 mV. Trace labelled Na^+ shows current recorded in Ringer solution; trace labelled TMA is the current recorded after substitution of TMA for Na^+; and trace labelled TTX is the current after addition (to Na^+ Ringer solution) of 200 nM-TTX. *B*, the peak transient current *vs.* command potential relationship is shown for the same cell as in *A*. The net Na^+ current was determined by subtracting the response to each voltage step in the presence of TTX from that recorded in the absence of the blocker. In this recording $R_a = 6{\cdot}6$ mΩ, $R_m = 410$ MΩ, and $C_m = 73{\cdot}6$ pF.

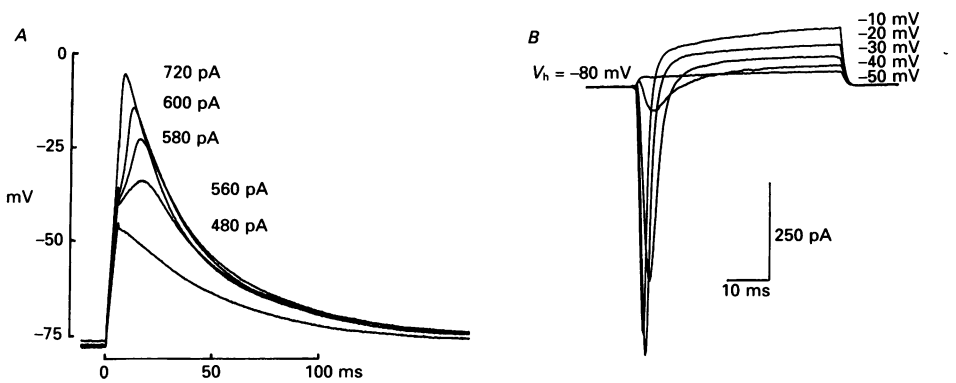

Fig. 7. *A*, action potentials recorded from a PCE cell. Recordings were made in current clamp. Cell was held at −80 mV by injecting a constant hyperpolarizing current. In response to injection of small depolarizing current pulses (e.g. 480 pA, 5 ms duration), cell showed a passive (capacitive) response with a time constant, $\tau = R_m C_m = 49{\cdot}1$ ms. For currents larger than 500 pA (5 ms duration) cell response was non-linear, indicating activation of regenerative currents. *B*, the DAIC recorded from the same cell under voltage clamp. Holding potential was −80 mV. Each trace is average of ten records. Transmembrane potentials during the 30 ms pulses are shown next to each trace. In this recording $R_a = 4{\cdot}4$ MΩ, $R_m = 646$ MΩ and $C_m = 76$ pF. The cell was superfused with Ringer solution.

perhaps also K^+ (140 mM). The TTX block was reversible (not shown). The relationship between the peak transient current and the command voltage for this cell is shown in Fig. 6*B*. For each command voltage, the peak transient Na^+ current was calculated by subtracting the current response in TTX-containing Ringer

solution (e.g. trace TTX in Fig. 6*A*) from that recorded in the absence of TTX (e.g. traces Na^+ and TMA in Fig. 6*A*). For such calculations, it was assumed that 200 nM-TTX blocks the DAIC completely.

While no spontaneous action potentials were recorded from the PCE cells, it was possible to elicit action potentials by injecting currents in the cells exhibiting DAIC. Figure 7*A* shows action potentials induced in a cell under current clamp. The transmembrane potential was held at about −80 mV by application of a steady current. The cell was then depolarized by injecting 5 ms current pulses, the amplitudes of which are shown next to each trace. Current pulses smaller than 500 pA failed to induce any regenerative response (e.g. lower trace for 480 pA). For such small current pulses, the membrane potential response seemed for the most part to be determined by the passive properties of the membrane. Large currents which brought the membrane potential above an apparent threshold of −45 mV induced action potentials whose size increased with injected current up to 600 pA. Because of the large size of this cell and small density of voltage-activated channels, the active component of the action potential was always smaller than its passive (capacitive) part. The peak Na^+ current in this cell was 690 pA (Fig. 7*B*), which implies a Na^+ current density of 9·1 $\mu A/cm^2$. The range of Na^+ current densities in twelve cells was 4·3 to 22·7 $\mu A/cm^2$ (12·5 ± 6·8, mean ± S.D.), compared with 20 to 100 $\mu A/cm^2$ in chromaffin cells (Marty & Neher, 1983) or 1 mA/cm^2 in the squid giant axon (Hodgkin & Huxley, 1952). Both action potentials and DAIC were reversibly blocked by 30 nM-TTX (not shown).

Hyperpolarization-activated current

In some PCE cells, hyperpolarization induced an inwardly rectified current (Fig. 8*A*). Because of the large size of this current, the maintenance of space and voltage clamp was not possible for most of the voltage range. The reason for this was that, for the largest current recorded, the specific membrane resistance (R_M) dropped to 702 Ω cm^2, and the voltage drop across the uncompensated series resistance reached 25·8 mV for a voltage pulse of −180 mV. However, it was still possible to investigate some properties of this current using whole-cell recording. One such property was the blocking effect of Ba^{2+}. After recording the family of current responses in Ringer solution shown in Fig. 8*A*, 2 mM-$BaCl_2$ was added to the superfusate. Responses to hyperpolarizing voltage steps to −150 mV from a holding potential of −80 mV declined rapidly (Fig. 8*B*) to about 2% of those recorded in Ringer solution before addition of Ba^{2+}. Figure 8*C* shows the family of responses recorded in presence Ba^{2+}. Recovery of the HAIC after removal of Ba^{2+} is shown in Fig. 8*D*. A similar block of HAIC was observed in solutions containing 1 mM-Cs^+ (not shown).

As with the DAOC, tail currents were used to determine the reversal potential for the HAIC (Fig. 9). The cell was held at −11 mV, hyperpolarized to a potential (−151 mV) large enough to open all inwardly rectifying channels but not to elicit any sag, and then lowered to different levels to record the tail currents. The duration of the hyperpolarizing pulse (50 ms) was chosen to be long enough to allow all the delayed rectifier channels that might have been open at −11 mV to close. The inset in Fig. 9 shows the same tail currents plotted at higher magnification. It appears that

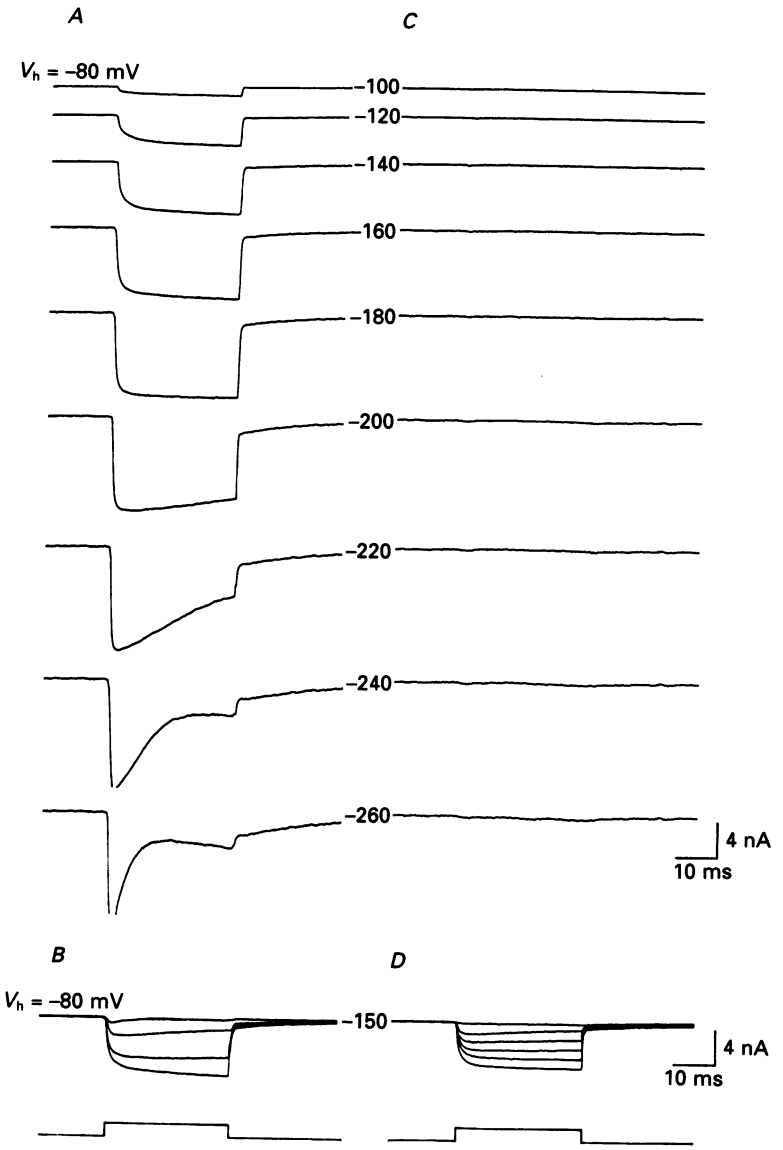

Fig. 8. The HAIC is blocked by Ba^{2+}. The hyperpolarization-activated currents were recorded from a PCE cell while superfusing with Ringer solution in the absence (*A*) and presence (*C*) of 2 mM-Ba^{2+}. Each trace is average of ten records. The values given near current traces are transmembrane potential (in mV) during the applied voltage steps. Holding potential, $V_h = -80$ mV. *B*, time course of suppression of the inwardly rectified current by Ba^{2+}. All traces are currents activated by a -70 mV pulse recorded at 30 s intervals during the onset of Ba^{2+} perfusion. *D*, recovery of the inwardly rectified current during wash-out of Ba^{2+}. Again, responses to -70 mV pulses, recorded at 30 s intervals, are shown. In this recording $R_a = 4{\cdot}1$ MΩ, $R_m = 100{\cdot}4$ MΩ, $C_m = 68{\cdot}9$ pF and R_a was 50 % compensated.

HAIC in this cell reverses at about −85 mV. For the cell in Fig. 9, using Goldman–Hodgkin–Katz equation we find a $P_{K/Na}$ valve of 127. For eight cells, $P_{K/Na}$ was calculated to be 130 ± 66. These results suggest that HAIC in PCE cells is carried by K^+ as in other tissues (Hille, 1984).

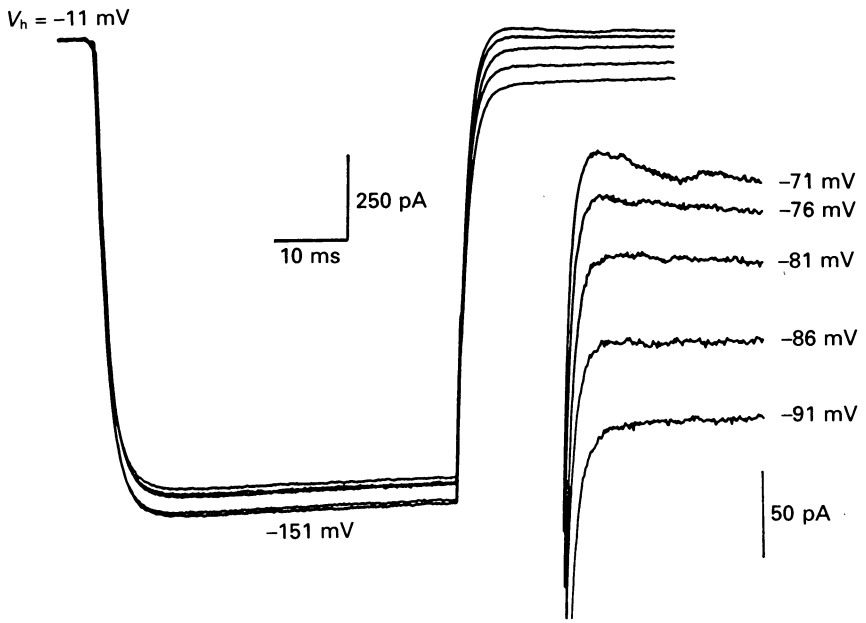

Fig. 9. Reversal potential of the HAIC determined by tail currents. For this cell, the holding potential was −11 mV, at which inwardly rectified currents were assumed to be absent. Hyperpolarizing voltage pulses 50 ms in duration to −151 mV were used to activate this conductance. At this potential level no sag was observed. The tail currents were recorded by repolarizing the cell to voltage levels between −91 and −71 mV. The tail currents are shown at a larger scale in the inset. Reversal potential for HAIC in this cell was about −85 mV. The cell was superfused during this recording with Ringer solution.

DISCUSSION

In order to investigate the membrane physiology of ciliary body epithelial cells, we have cultured the epithelium isolated from the stroma and the other tissues of the eye in a medium which we have previously shown to support the growth of pigmented (but not non-pigmented) ciliary body epithelial cells (Cilluffo *et al.* 1986). Recordings made exclusively from melanin-containing cell bodies show at least three types of voltage-activated conductances: an outwardly rectifying conductance activated by depolarization, selective for K^+ over Na^+, and blocked by TEA and Ba^{2+}; a transient depolarization-activated conductance selective for Na^+ and blocked by TTX; and a hyperpolarization-activated K^+ conductance blocked by external Ba^{2+} and Cs^+.

Depolarization-activated outward current

The DAOC in many respects resembles the delayed rectifier current observed in excitable tissues, for example in its delayed activation and sigmoidally shaped time course, its selectivity for K^+ over Na^+, its blockade by external TEA and Ba^{2+}, and its activation despite the presence of very low intracellular free Ca^{2+} concentration (*ca* 10^{-8} M). A similar K^+ current has been observed in single-channel recordings from the basolateral membrane of rabbit urinary bladder (Lewis & Hanrahan, 1985). A Ba^{2+}-blockable K^+ conductance in the basolateral membranes of both non-pigmented and pigmented ciliary epithelial cells of rabbit has been reported (Chu *et al.* 1986). Since it was not known if the isolated PCE cells grown in culture were polarized, the location of the voltage-activated channels in our cells could not be determined.

Depolarization-activated inward current

Our experiments provide the first demonstration of a TTX-blockable, voltage-activated Na^+ channel in a transporting epithelial cell from a mature vertebrate. Sodium currents have previously been demonstrated in transporting epithelia, but they are generally ligand modulated rather than voltage activated and are blocked by the pyrazine diuretic amiloride instead of TTX (For a review see Garty & Benos, 1988). Sodium currents similar in kinetics and pharmacology to those we have recorded in PCE cells have been shown to be present in sensory epithelia (e.g. taste receptor cells; Avenet & Lindemann, 1987). Sodium Na^+ channels blockable by TTX have also been described in several other cell types generally considered to be non-excitable, such as glial cells, some forms of T lymphocytes, and osteoblasts (see Chesnoy-Marchais & Fritsch, 1988).

The TTX-sensitive Na^+ conductance we have described in PCE cells appears to be similar to the one in muscle and nerve. Although the density of Na^+ channels is considerably smaller, it is large enough to permit the Na^+-dependent current of the ciliary body epithelial cells to become transiently net inward. As a result, these cells are capable of generating TTX-sensitive action potentials (see Figs 6 and 7). However, only 25% of the cells we tested contained any noticeable Na^+ conductance. This might have been due to the effect of enzymes we used for the cell dissociation, since the occurrence of cells with Na^+ currents seemed not to be entirely random. In some plates, none of the cells showed Na^+ channels, whereas in others every cell recorded from showed a net inward current. Furthermore, in some of our earlier experiments in which the epithelial tissue was dissociated with trypsin-containing medium, the percentage of cells possessing Na^+ current was even smaller (approximately 10%) than in the present experiments, in which the milder protease dispase was used. The small percentage of cells containing Na^+ channels might also have been due in part to an inhomogeneity of the PCE cell population. Our method of preparation provides epithelial cells from the entire ciliary body, and it is possible that there are functional differences in different areas of this tissue.

In some of our experiments, we noticed a residual DAIC in Na^+-free solutions or in Ringer solutions containing high concentrations of TTX (up to 1 μM). This current was small and infrequently observed, and we did not investigate it in detail. A Na^+-

independent inward current has also been recorded in bovine PCE cells, where it has been shown to be blocked by Cd^{2+} (and may therefore be carried by Ca^{2+}; Jacob, 1988).

Hyperpolarization-activated inward current

Some 13% of the PCE cells tested showed an HAIC which was selective for K^+ (Fig. 9) and blocked by Ba^{2+} (Fig. 8) and Cs^+ (not shown). Hyperpolarization-activated inward currents have been observed in whole-cell clamp recordings from the frog early distal tubule cells (Hunter, Oberleithner, Henderson & Giebisch, 1988), and there is evidence that they may be present in the basolateral membranes of *Necturus* proximal tubule cells (Hunter, Kawahara & Giebisch, 1986) and the apical membrane of *Amphiuma* early distal tubule cells (Kawahara, Hunter & Giebisch, 1986). Using the techniques described here, we were not able to localize the hyperpolarization-activated conductance to either of the PCE cell membranes.

One puzzling aspect of the HAIC in pigmented ciliary body epithelial cells is the presence of the sag in currents recorded in response to hyperpolarization to levels negative to −120 mV (Figs 3 and 8). A sag in the HAIC could be due to a voltage-dependent inactivation of the inwardly rectifying conductance (Almers, 1972; Sakmann & Trube, 1984), to potassium depletion in the mouth of the channels (Almers, 1972), or to channel block by one of the constituents of the Ringer solution (Ohmori, 1978). In preliminary experiments, complete replacement of the external Na^+ with K^+ led to removal of the sag in the HAICs (G. L. Fain & N. A. Farahbakhsh, unpublished observations; see also Gallin & McKinney, 1988, for a similar result in macrophages), though in some cells the size of the currents increased to the extent that they saturated our recording amplifier. Partial substitution of Na^+ by K^+ and partial or complete substitution by Li^+, choline or TMA had only minor effect on the kinetics of the sag. Removal of Ca^{2+}, Mg^{2+} or both had no effect. We have not been able to find a substitute for Na^+ other than K^+, for which the sag was completely removed. From our limited number of experiments, it would appear that K^+ depletion (either within the membrane infoldings or between the cell membrane and glass substrate) is the most likely explanation for the sag, though a role for external Na^+ block cannot be excluded.

Functional significance of voltage-activated conductances

Since epithelial cells are not usually thought to undergo large changes in membrane potential under physiological conditions, it might seem surprising that the pigmented cells of the ciliary body contain such a variety of voltage-activated conductances. Voltage-dependent K^+ conductances are present in many non-excitable cells and probably serve a variety of functions. Both inward and outward rectifiers stabilize the membrane potential at the K^+ equilibrium potential. These conductances could serve this function in an epithelium like the ciliary body, for which the cells are electrically coupled (Green *et al.* 1985), even if the K^+ channels were not present in all of the cells. Voltage-activated outward currents carried by K^+ have been postulated to participate in the volume regulatory decrease (VRD) following cell swelling (see for example Cahalan & Lewis, 1988). A component of VRD of the non-pigmented cells of ciliary body is mediated by a K^+ conductance,

since the rate of VRD can be altered by addition of Ba^{2+} or by changing extracellular K^+ concentration (Farahbakhsh & Fain, 1987). This may be true of the pigmented cells as well. In addition to their dependence upon transmembrane voltage, inwardly and outwardly rectifying K^+ conductances may also be modulated by pH (see for example Helbig *et al.* 1987) or cyclic nucleotides, which may in turn serve as internal messengers for hormones and circulating neuromodulators.

The most unexpected finding of our study is the presence of TTX-sensitive Na^+ channels in pigmented ciliary body epithelial cells. This finding raises the possibility that the electrically coupled cells of the ciliary body may be capable of conducting action potentials much as in the epithelia of some invertebrates (Anderson, 1980) and in the skin of tadpoles (Roberts & Stirling, 1971). We have shown that single pigmented cells are capable of generating Na^+-dependent spikes. However, Na^+ channels have not been found in all cells, and it is not yet clear whether the epithelium as a whole is capable of spike conduction. In invertebrates, epithelial conduction functions to synchronize activity among cells, in order to co-ordinate secretion, contraction, or luminescence (Anderson, 1980). It is unclear what purpose action potential conduction might serve in the ciliary body. It will be of considerable interest to investigate the distribution of Na^+ channels in this tissue, for example with monoclonal antibodies, and to study the function of Na^+ channels in monolayers of cultered pigmented ciliary body cells and in whole epithelium.

We are indebted to Dr Margery Fain and Marianne Cilluffo for the development of tissue culture methods and for growing the cells used in this study. We are also grateful to Dr Sally Krasne for commenting on the manuscript and Mr Harry Tillson for technical assistance. This work was supported by the National Eye Institute's grants EY 07568 to G.L.F., and EY 07026 and EY 06969 to N.A.F.

REFERENCES

ALMERS, W. (1972). Potassium conductance changes in skeletal muscle and the potassium concentration in the transverse tubules. *Journal of Physiology* **225**, 33–56.

ANDERSON, P. A. V. (1980). Epithelial conduction: its properties and functions. *Progress in Neurobiology* **15**, 161–203.

AVENET, P. & LINDEMANN, B. (1987). Patch-clamp study of isolated taste receptor cells of the frog. *Journal of Membrane Biology* **97**, 223–240.

BEZANILLA, F. (1985). A high capacity data recording device based on a digital audio processor and a video cassette recorder. *Biophysical Journal* **47**, 437–441.

BIANCHI, C., ANAND-SRIVASTAVA, M. D., DE LEAN, A., GUTKOWSKA, J., FORTHOMME, D., GENEST, J. & CANTIN, M. (1986). Localization and characterization of specific receptors for atrial natriuretic factor in the ciliary processes of the eye. *Current Eye Research* **5**, 283–293.

BILL, A. (1973). The role of ciliary blood flow and ultrafiltration in aqueous humor formation. *Experimental Eye Research* **16**, 287–298.

CAHALAN, M. D. & LEWIS, R. S. (1988). Role of potassium and chloride channels in volume regulation by T lymphocytes. In *Cell Physiology of Blood*, ed. GUNN, R. B. & PARKER, J. C., pp. 281–301. New York: Rockefeller University Press.

CHESNOY-MARCHAIS, D. & FRITSCH, J. (1988). Voltage-gated sodium and calcium currents in rat osteoblasts. *Journal of Physiology* **398**, 291–311.

CHU, T.-C., CANDIA, O. A. & IIZUKA, S. (1986). Effects of forskolin, prostoglandin $F_{2\alpha}$, and Ba^{2+} on the short-circuit current of the isolated rabbit iris-ciliary body. *Current Eye Research* **5**, 511–516.

CILLUFFO, M. C., FAIN, M. J., FAIN, G. L. & BRECHA, N. C. (1986). Culture of rabbit ciliary body epithelium. *Investigative Ophthalmology and Visual Science* **27**, suppl., 322.

CILLUFFO, M. C., FAIN, M. J., FARAHBAKHSH, N. A., FAIN, G. L. & LEE, D. A. (1988). Rabbit

ciliary body epithelial cells grown on porous membranes. *Investigative Ophthalmology and Visual Science* **29**, suppl., 86.

COLE, D. A. (1984). Ocular fluids. In *The Eye*, vol. 1A, *Vegetative Physiology and Biochemistry*, 3rd edn, ed. DAVSON, H., pp. 269–390. New York: Academic Press.

FAIN, G. L., SMOLKA, A., CILLUFFO, M. C., FAIN, M. J., LEE, D. A., BRECHA, N. C. & SACHS, G. (1988). Monoclonal antibodies to the H^+–K^+ ATPase of gastric mucosa selectively stain the non-pigmented cells of the rabbit ciliary body epithelium. *Investigative Ophthalmology and Visual Science* **29**, 785–794.

FARAHBAKHSH, N. A. & FAIN, G. L. (1987). Volume regulation of non-pigmented cells from ciliary epithelium. *Investigative Ophthalmology and Visual Science* **28**, 934–944.

FARAHBAKHSH, N. A., FAIN, M. J. & FAIN, G. L. (1987). Patch-clamp recordings from rabbit pigmented ciliary epithelial cells grown in culture. *Investigative Ophthalmology and Visual Science* **28**, suppl., 76.

FENWICK, E. M., MARTY, A. & NEHER, E. (1982). Sodium and calcium channels in bovine chromaffin cells. *Journal of Physiology* **331**, 577–597.

FISCHMEISTER, R., AYER, R. K. & DEHAAN, R. L. (1986). Some limitations of the cell-attached patch clamp technique: a two-electrode analysis. *Pflügers Archiv* **406**, 73–82.

FRÖMTER, E. (1972). The route of passive ion movement through the epithelium of *Necturus* gall bladder. *Journal of Membrane Biology* **8**, 259–301.

GALLIN, E. K. & MCKINNEY, L. C. (1988). Potassium conductances in macrophages. In *Cell Physiology of Blood*, ed. GUNN, R. B. & PARKER, J. C., pp. 315–332. New York: Rockefeller University Press.

GARTY, H. & BENOS, D. J. (1988). Characteristics and regulatory mechanisms of the amiloride-blockable Na^+ channel. *Physiological Reviews* **68**, 309–373.

GREEN, K., BOUNTRA, C., GEORGIOU, P. & HOUSE, C. R. (1985). An electrophysiologic study of rabbit ciliary epithelium. *Investigative Ophthalmology and Visual Science* **26**, 371–381.

HAGIWARA, S. & OHMORI, H. (1982). Studies of calcium channels in rat clonal pituitary cells with patch electrode voltage clamp. *Journal of Physiology* **331**, 231–252.

HAMILL, O. P., MARTY, A., NEHER, E., SAKMANN, B. & SIGWORTH, F. J. (1981). Improved patch-clamp technique for high-resolution current recording from cell and cell-free membrane patches. *Pflügers Archiv* **391**, 85–100.

HELBIG, H., KORBMACHER, C. & WIEDERHOLT, M. (1987). K^+-conductance and electrogenic Na^+/K^+ transport of cultured bovine pigmented ciliary epithelium. *Journal of Membrane Biology* **99**, 173–186.

HILLE, B. (1984). *Ionic Channels of Excitable Membranes*. Sunderland, MA, USA: Sinauer Associates Inc.

HODGKIN, A. L. & HUXLEY, A. F. (1952). A quantitative description of membrane current and its application to conduction and excitation in nerve. *Journal of Physiology* **117**, 500–544.

HODGKIN, A. L., MCNAUGHTON, P. A., NUNN, B. J. & YAU, K.-W. (1984). Effects of ions on retinal rods from *Bufo marinus*. *Journal of Physiology* **350**, 649–680.

HUNTER, M., KAWAHARA, K. & GIEBISCH, G. (1986). Potassium channels along the nephron. *Federation Proceedings* **45**, 2723–2726.

HUNTER, M., OBERLEITHNER, H., HENDERSON, R. M. & GIEBISCH, G. (1988). Whole-cell potassium currents in single early distal tubule cells. *American Journal of Physiology* **255** (*Renal Fluid Electrolyte Physiology* 24), F699–703.

JACK, J. J. B., NOBLE, D. & TSIEN, R. W. (1975). *Electric currents in excitable cells*. London: Oxford University Press.

JACOB, T. J. C. (1988). Inward and outward currents in isolated epithelial cells of the bovine ciliary body. *Journal of Physiology* **407**, 103*P*.

JOYNER, R. W., MOORE, J. W. & RAMONE, F. (1975). Axon voltage-clamp simulation. III. Postsynaptic region. *Biophysical Journal* **15**, 37–54.

KAWAHARA, K., HUNTER, M. & GIEBISCH, G. (1986). Potassium and chloride channels in the luminal and basolateral membranes of *Amphiuma* early distal tubule. *Kidney International* **29**, 399.

LEWIS, S. A. & HANRAHAN, J. W. (1985). Apical and basolateral membrane ionic channels in rabbit urinary bladder epithelium. *Pflügers Archiv* **405**, suppl. 1, S83–88.

LINDAU, M. & NEHER, E. (1988). Patch-clamp techniques for time-resolved capacitance measurements in single cells. *Pflügers Archiv* **411**, 137–146.

MARTY, A. & NEHER, E. (1983). Tight-seal whole-cell recording. In *Single-Channel Recording*, ed. SAKMANN, B. & NEHER, E., pp. 107–122. New York: Plenum Press.

OHMORI, H. (1978). Inactivation kinetics and steady-state current noise in the anomalous rectifier of tunicate egg cell membranes. *Journal of Physiology* **281**, 77–99.

RAVIOLA, G. & RAVIOLA, R. (1978). Intercellular junctions in the ciliary epithelium. *Investigative Ophthalmology and Visual Science* **17**, 958–981.

ROBERTS, A. & STIRLING, C. A. (1971). The properties and propagation of a cardiac-like impulse of the skin of young tadpoles. *Zeitschrift für vergleichende Physiologie* **71**, 295–310.

SAKMANN, B. & TRUBE, G. (1984). Voltage-dependent inactivation of inward-rectifying single-channel currents in the guinea-pig heart cell membrane. *Journal of Physiology* **347**, 659–683.

STANFIELD, P. R. (1983). Tetraethylammonium ions and potassium permeability of excitable cells. *Reviews of Physiology Biochemistry and Pharmacology* **97**, 1–67.

STIMERS, J. R., BEZANILLA, F. & TAYLOR, R. E. (1987). Sodium channel gating currents. *Journal of General Physiology* **89**, 521–540.

TAYLOR, R. E., MOORE, J. W. & COLE, K. S. (1960). Analysis of certain errors in squid axon voltage clamp measurements. *Biophysical Journal* **1**, 161–202.

TESSIER-LAVIGNE, M., ATTWELL, D., MOBBS, P. & WILSON, M. (1988). Membrane currents in retinal bipolar cells of the axolotl. *Journal of General Physiology* **91**, 49–72.